DOI:10.3969/J.ISSN.100-5137.2017.03.011

Some new observations for a stage-structured predator–prey model

Li Wei, Li Xianyi*

(Department of Big Data Science, College of Science, Zhejiang University of Science and Technology, Hangzhou 310023, China)

Abstract: A 3D stage–structured predator–prey model, whose necessary and sufficient conditions for the permanence of two species and the extinction of one species or two species were previously obtained, is revisited in this paper. By using the center manifold theorem, we show that the nonnegative equilibrium point of this system is also locally asymptotically stable in the critical case $a = b + ce$. Our main new discovery is that the parameter d in this model irrelevant to finite dynamical behaviors of this system plays a role in the dynamical behaviors at infinity of this system. More specially, by using the Poincaré compactication in $\mathbb{R}^3$ we make a global analysis for this model, including the complete description of its dynamic behavior on the sphere at infinity. Combining analytical and numerical techniques we show that for the parameters satisfying $a \leqslant b$ and $0 < d < 1$, the system presents two infinite heteroclinic orbits.

Key words: stage–structured predator–prey model; center manifold theorem; dynamics at infinity; Poincaré compactification; infinite heteroclinic orbit

CLC number: O 175.13 **Document code:** A **Article ID:** 1000-5137(2017)03-0422-10

2010 MSC: 34C45, 34C37, 34D20

关于一阶段结构捕食模型的新观察

李　蔚，李先义 *

(浙江科技学院 理学院 大数据科学系，杭州 310023)

摘　要：重访一 3 维阶段构造模型，它的两种群持久和一种群或者两种群灭绝的必要充分条件先前已经得到．通过使用中心流型定理，证明这个系统的非负平衡点在临界状态 $a = b + ce$ 时也是局部渐近稳定的．主要新的发现是：系统中与有限动力学无关的参数 d 在系统的无穷远动力学中担任一个关键角色．更具体地，通过在 $\mathbb{R}^3$ 中使用庞加莱紧性法，对该模型的性质做了一个全局分析，包括在无穷远球面上动力学的完

Received date: 2017-03-21

Foundation item: This research was supported by the Natural Science Foundation (NSF) of Zhejiang Province (No. LQ13A01 0019); NSF of China (No. 61473340); NSF of Zhejiang University of Science and Technology (No. F701108G14).

$*$**Corresponding author:** Li Xianyi, professor, reseach area: ordinary differential equation and dynamical system, E-mail: mathxyli@zust.edu.cn

整描述．组合解析与数值的技术，证明了在参数满足 $a \leqslant b$ 且 $0 < d < 1$ 的条件下，系统具有两条无穷远异宿轨．

关键词：阶段结构捕食模型；中心流型定理；无穷远动力学；庞加莱紧性法；无穷异宿轨

1 Introduction

It is known to all that the predator–prey models have been extensively studied by many researchers[1−10] in recent years, whose permanence (or strong persistence) and extinction are important contents of investigations. Almost all animals have the stage structure of immature and mature in real biological world. So the related models with stage structure are more closely aligned with the objective facts. Recently, those papers[11−13] studied the stage structure of species with or without time delays. Most of them considered the finite behaviors for those models. However, the dynamical behaviors at infinity of those models are not known at all. One has now seen that the dynamics at infinity of a given model is an interesting and important topic[14−20], especially with the biological meanings of a biological system. Therefore, in this paper, our step goes on toward this orientation- the dynamics at infinity of a given model.

Our main work is to make a global analysis for the following stage-structured predator–prey model

$$\begin{cases} \dot{x} &= ay - bx - cx^2 - dxz, \\ \dot{y} &= x - y, \\ \dot{z} &= z(-e + x - z), \end{cases} \tag{1}$$

which is presented in [21], and where the parameters $(a, b, c, d, e) \in {\mathbb{R}^+}^5$ are all positive real numbers due to their biological meanings.

Although the authors in [21] did not give the detailed conditions for the existence of equilibrium of system (1), one can easily derive the following proposition.

Proposition 1 For the parameters $(a, b, c, d, e) \in {\mathbb{R}^+}^5$, system (1) has always the equilibrium point $O(0, 0, 0)$. Furthermore, one has:

(1) If $a \leqslant b$, then the origin O is the unique equilibrium point of system (1);

(2) If $b < a \leqslant b + ce$, then system (1) has two equilibria. Namely, besides the origin O there is a non-negative equilibrium $E_1\Big(\dfrac{a-b}{c}, \dfrac{a-b}{c}, 0\Big)$;

(3) If $a > b + ce$, then system (1) has three equilibria, i.e., except the origin O and the non-negative equilibrium E_1, there is also a positive equilibrium $E_2\Big(\dfrac{a-b+de}{c+d}, \dfrac{a-b+de}{c+d}, \dfrac{a-b-ce}{c+d}\Big)$.

Some dynamics of three equilibria have been considered in [21] and the local dynamics of the three equilibria are first presented. For the non-negative equilibrium E_1, the result is:

Result 1 [21] $E_1\Big(\dfrac{a-b}{c}, \dfrac{a-b}{c}, 0\Big)$ is a saddle with $\mathrm{dim}W^u(E_1) = 1$, $\mathrm{dim}W^s(E_1) = 2$ for $a > b + ce$; E_1 is globally asymptotically stable for $b < a < b + ce$.

How about the local stability of equilibrium E_1 in the critical case $a = b + ce$? This has not been answered yet in the known literature. So, in the sequel, we will first solve this problem by using the center manifold theorem. Although the global stability of equilibrium E_1 in the critical case $a = b + ce$ is solved by using Lyapunov function and LaSalle theorem, our method is different from the one used in [21]. So, our method may be also regarded as a complementary method.

For the global dynamics of the three equilibria, some results are obtained as follows.

Result 2 [21] If $a > b + ce$, then the positive equilibrium E_2 of system (1) is globally asymptotically stable. If $b < a < b + ce$, then the non-negative equilibrium E_1 of system (1) is globally asymptotically stable. If $a \leqslant b$, then the origin O of system (1) is globally asymptotically stable.

The numerical simulations performed also confirm these theoretical results, for example, see Fig. 1.

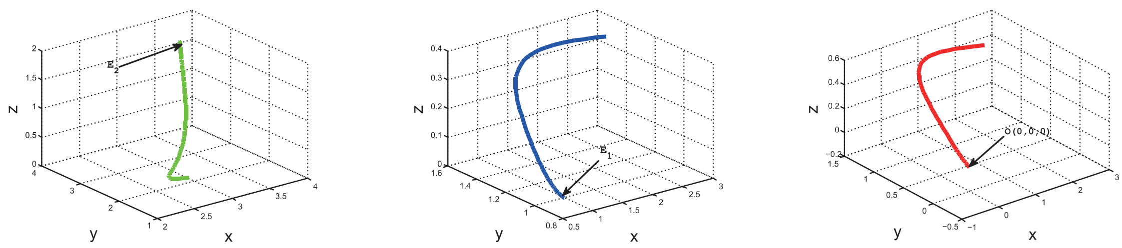

(a) $(a, b, c, d, e) = (10, 1, 2, 1, 2)$ (b) $(a, b, c, d, e) = (3, 1, 2, 1, 2)$ (c) $(a, b, c, d, e) = (1, 2, 1, 1, 1)$

Figure 1 Phase portrait of system (1) with the same initial value $(x_0, y_0, z_0) = (2.618, 1.382, 0.382)$ and the parameters satisfying: (a) $a > b + ce$, (b) $b < a \leqslant b + ce$, (c) $a \leqslant b$

By careful observations, one finds that, the above Result 2 for the global dynamics of system (1) is only related to its parameters a, b, c and e, not the parameter d. That is to say, the parameter d has nothing to do with the global stability of this system. Then, what role does the parameter d play in the dynamics of system (1)? Because system (1) is derived from a real biological model by a dimensionless change, the parameter d, if returned to its original system, corresponds to some biological factors. Since it is related to biological factors, it must affect something of the population. Therefore, a natural question "Has system (1) been explored thoroughly?" comes out in our mind. It seems that the answer is not obvious. But one can easily find that Result 2 is only concerned with its finite dynamical behaviors. That is to say, its dynamics at infinity has not been investigated yet. So, one naturally conjectures: The parameter d effects the behaviors at infinity of system (1). Indeed, it is proved in the sequel that the conjecture is true.

The system (1) can be extended to an analytic system on a closed ball of radius one, whose interior is diffeomorphic to $\mathbb{R}^3$ and whose invariant boundary, by the extended flow, is a 2-dimensional sphere $\mathbb{S}^2$ and plays the role of the infinity. The technique for making such an extension is precisely the Poincaré compactification and is described in detail in Section 3. It will be used here for studying the dynamics of system (1) in a neighborhood of infinity and on the sphere at infinity.

Our main results in this paper are summarized in the following two theorems.

Theorem 1 For the parameters $(a, b, c, d, e) \in \mathbb{R}^{+5}$, for the infinite equilibria at coordinate axes of system (1), we have the following conclusions:

1. The two equilibria in the positive and negative endpoints of the x–axis are two unstable nodes.

2. The two equilibria in the positive and negative endpoints of the y–axis are two centers.

Furthermore, the following statements hold:

(i) If $0 < d < 1$, the two equilibria in the positive and negative endpoints of the z–axis are two saddle–nodes, there still are infinitely many saddle–node points with a 1D W^s_{loc} and a 2D W^u_{loc} respectively.

(ii) If $d \geqslant 1$, the two non-hyperbolic equilibria in the positive and negative endpoints of the z–axis are all unstable with a 1D W^s_{loc} and a 2D W^u_{loc}, too.

For the phase portrait of system (1) on the sphere at infinity, see Fig. 2.

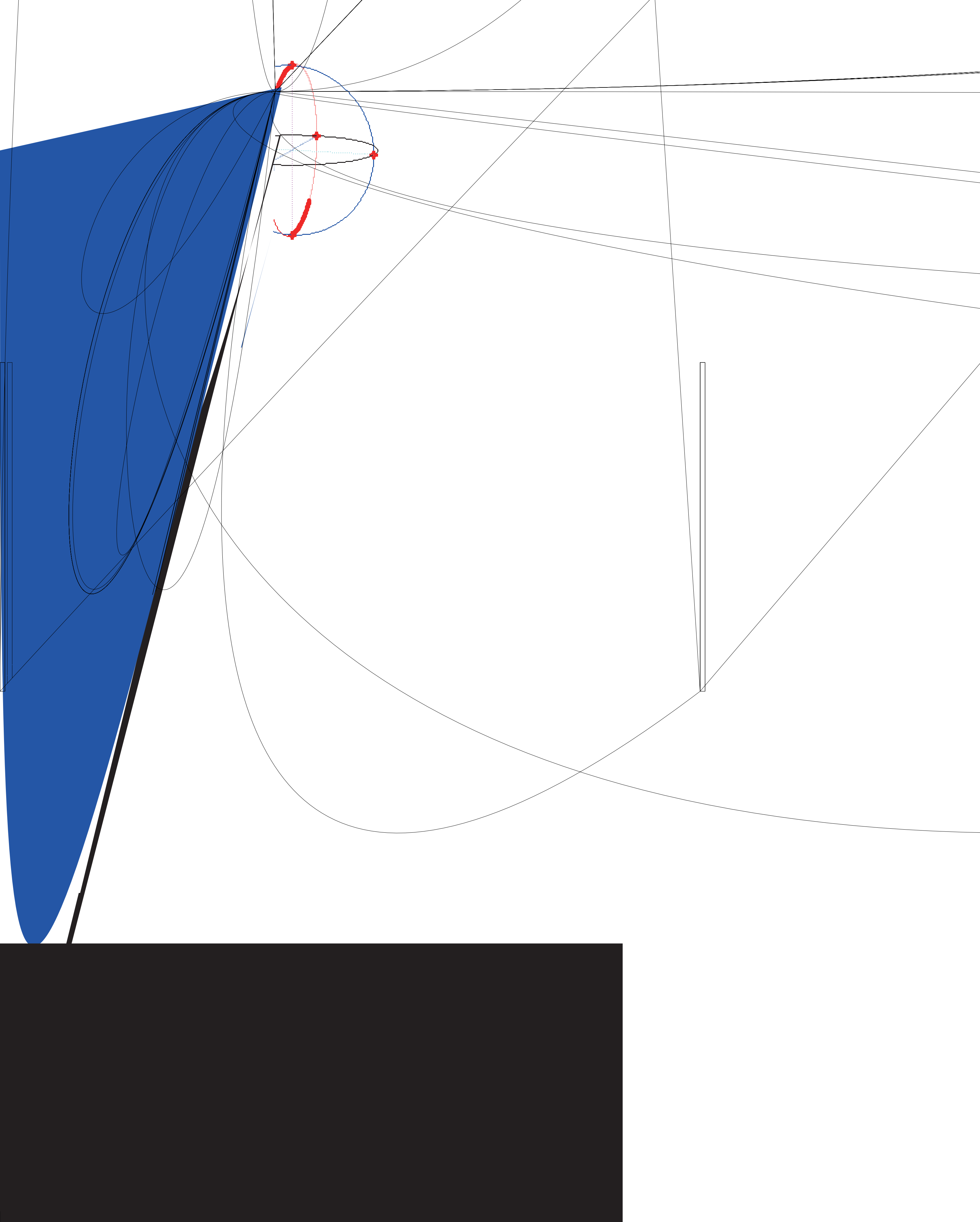

2 Local stability of equilibrium E_1 in the critical case $a = b + ce$

For the local stability of equilibrium E_1 in the critical case $a = b + ce$, one has the following results.

Theorem 3 The equilibrium E_1 of the system (1) is locally asymptotically stable in the critical case $a = b+ce$.

Proof In the critical case $a = b+ce$, E_1 reduces to $E_1(e, e, 0)$. Take the change $x_1 = x-e$, $x_2 = y-e$, $x_3 = z-0$, which transforms the system (1) into

$$\begin{cases} \dot{x}_1 = ax_2 - (b+2ce)x_1 - edx_3 - cx_1^2 - dx_1x_3, \\ \dot{x}_2 = x_1 - x_2, \\ \dot{x}_3 = x_3(x_1 - x_3), \end{cases} \tag{2}$$

and E_1 to the origin O. The corresponding Jacobian matrix is

$$\begin{pmatrix} -b-2ce & a & -de \\ 1 & -1 & 0 \\ 0 & 0 & 0 \end{pmatrix}$$

with an eigenvalue 0. So, O is then a center. According to the center manifold theory, the stability of O can be determined by studying a first-order ordinary differential equation on a center manifold, which can be represented as a graph for the variable x_3 as follows

$$W^c_{loc}(O) = \left\{ \begin{pmatrix} x_1 \\ x_2 \\ x_3 \end{pmatrix} \middle| \begin{array}{l} |x_3| < \delta, \\ x_1 = h_1(x_3), h_1(0) = 0, \\ x_2 = h_2(x_3), h_2(0) = 0 \end{array} \right\}$$

with δ sufficiently small.

Assume that $x_1 = h_1(x_3) = a_0x_3 + a_1x_3^2 + O(x_3^3)$ and $x_2 = h_2(x_3) = b_0x_3 + b_1x_3^2 + O(x_3^3)$. Then, the center manifold must satisfy

$$\begin{array}{l} h_1'(x_3)x_3(x_1 - x_3) = ax_2 - (b+2ce)x_1 - edx_3 - cx_1^2 - dx_1x_3, \\ h_2'(x_3)x_3(x_1 - x_3) = x_1 - x_2. \end{array}$$

From this, one obtains that

$$h_1(x_3) = -\frac{d}{c}x_3 + \frac{d(c+d)(b+ce+1-c)}{c^3e}x_3^2 + O(x_3^3)$$

and

$$h_2(x_3) = -\frac{d}{c}x_3 - \frac{d(c+d)(b+2ce+1-c)}{c^3e}x_3^2 + O(x_3^3).$$

Hence, the vector field is reduced to the center manifold

$$\dot{x_3} = -\frac{c+d}{c}x_3^2 + O(x_3^3). \tag{3}$$

By the known assumption $c > 0$ and $d > 0$, it follows from (3) that $x_3 \to 0$ for $t \to +\infty$. Thus, $(x_1\, x_2, x_3)$ in the system (2) tends to $(0, 0, 0)$ when $t \to +\infty$. This imples that the origin O of the system (2) is asymptotically stable and thus the equilibrium E_1 of the system (1) is locally asymptotically stable.

3 Poincaré compactification in $\mathbb{R}^3$

A polynomial vector field X in $\mathbb{R}^n$ can be extended to a unique analytic vector field on the sphere $\mathbb{S}^n$. The technique for making such an extension is called the Poincaré compactification and allows us to study a polynomial vector field in a neighborhood of infinity, which corresponds to the equator $\mathbb{S}^{n-1}$ of the sphere $\mathbb{S}^n$. Poincaré introduced this compactification for polynomial vector fields in $\mathbb{R}^2$. Its extension to $\mathbb{R}^n$ for $n > 2$ can be found in [20]. We here describe the Poincaré compactification for polynomial vector fields in $\mathbb{R}^3$ following closely[20].

In $\mathbb{R}^3$ we consider the polynomial differential system

$$\dot{x} = P^1(x, y, z), \quad \dot{y} = P^2(x, y, z), \quad \dot{z} = P^3(x, y, z),$$

or equivalently its associated polynomial vector field $X = (P^1, P^2, P^3)$. The degree n of X is defined as $n = \max\{\deg(P^i) : i = 1, 2, 3\}$.

Let $\mathbb{S}^3 = \{y = (y_1, y_2, y_3, y_4) \in \mathbb{R}^4 : \|y\| = 1\}$ be the unit sphere in $\mathbb{R}^4$, and $S_+ = \{y \in \mathbb{S}^3 : y_4 > 0\}$ and $S_- = \{y \in \mathbb{S}^3 : y_4 < 0\}$ be the northern and southern hemispheres of $\mathbb{S}^3$, respectively. The tangent space to $\mathbb{S}^3$ at the point y is denoted by $T_y\mathbb{S}^3$. Then the tangent plane

$$T_{(0,0,0,1)}\mathbb{S}^3 = \{(x_1, x_2, x_3, 1) \in \mathbb{R}^4 : (x_1, x_2, x_3) \in \mathbb{R}^3\}$$

is identified with $\mathbb{R}^3$.

We consider the central projections $f_+ : \mathbb{R}^3 = T_{(0,0,0,1)}\mathbb{S}^3 \to \mathbb{S}_+$ and $f_- : \mathbb{R}^3 = T_{(0,0,0,1)}\mathbb{S}^3 \to \mathbb{S}_-$ defined by $f_\pm(x) = \pm(x_1, x_2, x_3, 1)/\Delta x$, where $\Delta x = (1 + \Sigma_{i=1}^3 x_i^2)^{\frac{1}{2}}$. Through these central projections $\mathbb{R}^3$ is identified with the northern and southern hemispheres. The equator of $\mathbb{S}^3$ is $\mathbb{S}^2 = \{y \in \mathbb{S}^3 : y_4 = 0\}$. Clearly $\mathbb{S}^2$ can be identified with the infinity of $\mathbb{R}^3$.

The maps f_+ and f_- define two copies of X on $\mathbb{S}^3$, one $Df_+ \circ X$ in the northern hemisphere and the other $Df_- \circ X$ in the southern one. Denote by $\bar{X}$ the vector field on $\mathbb{S}^3 \backslash \mathbb{S}^2 = \mathbb{S}_+ \cup \mathbb{S}_-$,which, restricted to $\mathbb{S}_+$ coincides with $Df_+ \circ X$ and restricted to $\mathbb{S}_-$ coincides with $Df_- \circ X$.

The expression for $\overline{X}(y)$ on $\mathbb{S}_+ \cup \mathbb{S}_-$ is

$$\overline{X}(y) = y_4 \begin{pmatrix} 1 - y_1^2 & -y_2 y_1 & -y_3 y_1 \\ -y_1 y_2 & 1 - y_2^2 & -y_3 y_2 \\ -y_1 y_3 & -y_2 y_3 & 1 - y_3^2 \\ -y_1 y_4 & -y_2 y_4 & -y_3 y_4 \end{pmatrix} \begin{pmatrix} P^1 \\ P^2 \\ P^3 \end{pmatrix},$$

where $P^i = P^i(y_1/|y_4|, y_2/|y_4|, y_3/|y_4|)$. Written in this way $\overline{X}(y)$ is a vector field in $\mathbb{R}^4$ tangent to the sphere $\mathbb{S}^3$.

Now we can analytically extend the vector field $\overline{X}(y)$ to the whole sphere $\mathbb{S}^3$ by considering $p(X)(y) = y_4^{n-1}\overline{X}(y)$, where n is the degree of X. This extended vector field $p(X)$ is called the Poincaré compactification of X on $\mathbb{R}^3$.

As $\mathbb{S}^3$ is a differentiable manifold, in order to compute the expression for $p(X)$ we can consider the eight local charts (U_i, F_i), (V_i, G_i), where $U_i = \{y \in \mathbb{S}^3 : y_i > 0\}$ and $V_i = \{y \in \mathbb{S}^3 : y_i < 0\}$ for $i = 1, 2, 3, 4$ are the inverses of the central projections from the origin to the tangent planes at the points $(\pm1, 0, 0, 0)$, $(0, \pm1, 0, 0)$, $(0, 0, \pm1, 0)$ and $(0, 0, 0, \pm1)$, respectively. Now we do the computations on U_1. Suppose that the origin $(0, 0, 0, 0)$, the point $(y_1, y_2, y_3, y_4) \in \mathbb{S}^3$ and the point $(1, z_1, z_2, z_3)$ in the tangent plane to $\mathbb{S}^3$ at $(1, 0, 0, 0)$ are collinear. Then we have $1/y_1 = z_1/y_2 = z_2/y_3 = z_3/y_4$, and consequently $F_1(y) = (y_2/y_1, y_3/y_1, y_4/y_1) = (z_1, z_2, z_3)$ defines the coordinates on U_1. As

$$DF_1(y) = \begin{pmatrix} -y_2/y_1^2 & 1/y_1 & 0 & 0 \\ -y_3/y_1^2 & 0 & 1/y_1 & 0 \\ -y_4/y_1^2 & 0 & 0 & 1/y_1 \end{pmatrix}$$

and $y_4^{n-1} = (z_3/\Delta z)^{n-1}$, the analytical vector field $p(X)$ becomes

$$\frac{z_3^n}{(\Delta z)^{n-1}}(-z_1 P^1 + P^2, -z_2 P^1 + P^3, -z_3 P^1),$$

where $P^i = P^i(1/z_3, z_1/z_3, z_2/z_3)$.

In a similar way we can deduce the expressions of $p(X)$ in U_2 and U_3. These are

$$\frac{z_3^n}{(\Delta z)^{n-1}}(-z_1 P^2 + P^1, -z_2 P^2 + P^3, -z_3 P^2),$$

where $P^i = P^i(z_1/z_3, 1/z_3, z_2/z_3)$ in U_2, and

$$\frac{z_3^n}{(\Delta z)^{n-1}}(-z_1P^3 + P^1, -z_2P^3 + P^2, -z_3P^3),$$

where $P^i = P^i(z_1/z_3, z_2/z_3, 1/z_3)$ in U_3.

The expression for $p(X)$ in U_4 is $z_3^{n+1}(P^1, P^2, P^3)$ where $P^i = P^i(z_1, z_2, z_3)$. The expression for $p(X)$ in the local chart V_i is the same as in U_i multiplied by $(-1)^{n-1}$.

When we work with the expression of the compactified vector field $p(X)$ in the local charts we shall omit the factor $1/(\Delta z)^{n-1}$. We can do that through a rescaling of the time variable.

Next we shall work with the orthogonal projection of $p(X)$ from the closed northern hemisphere to $y_4 = 0$, and we continue denoting this projected vector field by $p(X)$. Note that the projection of the closed northern hemisphere is a closed ball $\boldsymbol{B}$ of radius one, whose interior is diffeomorphic to $\mathbb{R}^3$ and whose boundary $\mathbb{S}^2$ corresponds to the infinity of $\mathbb{R}^3$. Of course $p(X)$ is defined in the whole closed ball $\boldsymbol{B}$ in such a way that the flow on the boundary is invariant. This new vector field on $\boldsymbol{B}$ will be called the Poincaré compactification of X, and $\boldsymbol{B}$ will be called the Poincaré ball.

Remark 1 All the points on the invariant sphere $\mathbb{S}^2$ at infinity in the coordinates of any local chart U_i and V_i have $z_3 = 0$. Also, the points in the interior of the Poincaré ball, which is diffeomorphic to $\mathbb{R}^3$, are given in the local charts U_1, U_2 and U_3 by $z_3 > 0$ and in the local charts V_1, V_2 and V_3 by $z_3 < 0$.

4 Dynamical behavior of system (1) at infinity

In this section, we shall make an analysis of the flow of system (1) near and at infinity.

This section is divided into three subsections: in Subsection 4.1 we study the dynamics of system (1) near infinity; in Subsection 4.2, we consider the dynamics of system (1) at infinity and consequently prove Theorem 1. Based on the knowledge of the dynamical behavior near and at infinity, in Subsection 4.3 we prove Theorem 2.

4.1 Dynamical behavior of system (1) near infinity

In this subsection we shall analyze the flow of system (1) near and at infinity. In order to do so, in the following three subsections, we shall analyze the Poincaré compactification of system (1) in the local charts U_i and V_i, $i = 1, 2, 3$.

4.1.1 In the local charts U_1 and V_1

According to the method in Section 3, the expression of the Poincaré compactification $p(X)$ of system (1) in the local chart U_1 is given by

$$\begin{cases} \dot{z_1} &= -az_1^2z_3 + (b-1)z_1z_3 + z_3 + cz_1 + dz_1z_2, \\ \dot{z_2} &= -az_1z_2z_3 + (b-e)z_2z_3 + (d-1)z_2^2 + (c+1)z_2, \\ \dot{z_3} &= -az_1z_3^2 + bz_3^2 + cz_3 + dz_2z_3. \end{cases} \tag{4}$$

Taking $z_3 = 0$ (which corresponds to the points on the sphere $\mathbb{S}^2$ at infinity), system (4) is reduced to the system as follows

$$\begin{cases} \dot{z_1} &= z_1(c + dz_2), \\ \dot{z_2} &= z_2[(d-1)z_2 + (c+1)]. \end{cases} \tag{5}$$

Since $d > 0$, we may consider two cases: (i) $d = 1$, (ii) $d \neq 1$.

(i) If $d = 1$, then system (4) has a unique equilibrium point $I_0(0, 0, 0)$, and the corresponding three eigenvalues are $\lambda_{1,3} = c$ and $\lambda_2 = c + 1$. Hence, I_0 is an unstable node because $c > 0$.

(ii) If $d \neq 1$, then $I_1\Big(0, \dfrac{1+c}{1-d}, 0\Big)$ is the other equilibrium point of system (4) in addition to I_0. The three eigenvalues of the linear part of system (4) at I_1 are $\lambda_{1,3} = \dfrac{c+d}{1-d}$ and $\lambda_2 = -(c+1)$. Therefore, one can see that I_1 is a saddle-node for $0 < d < 1$, and a stable node for $d > 1$.

The flow in the local chart V_1 is the same as the flow in the local chart U_1, because the compactified vector field $p(X)$ in V_1 coincides with the vector field $p(X)$ in U_1 multiplied by $(-1)^{n-1}$, where $n = 2$ is the degree of system (1) (for details see Section 3). Therefore, the above analysis holds for the flow in the local chart V_1 .

4.1.2 In the local charts U_2 and V_2

Again using the method in Section 3 we have the expression of the Poincaré compactification $p(X)$ of system (4) in the local chart U_2 as follows

$$\begin{cases} \dot{z_1} &= -z_1^2 z_3 + (1-b)z_1 z_3 + a z_3 - c z_1^2 - d z_1 z_2, \\ \dot{z_2} &= -z_1 z_2 z_3 + (1-e) z_2 z_3 + z_1 z_2 - z_2^2, \\ \dot{z_3} &= -z_1 z_3^2 + z_3^2. \end{cases} \tag{6}$$

Notice $z_3 = 0$ implies that system (6) has a unique equilibrium point I_0 with three null eigenvalues. Let us try to understand the flow near the equilibrium. From the compactification procedure described in Section 3 we know that the $z_1 z_2$–plane is invariant under the flow of system (6), so we can completely describe the dynamics on the sphere at infinity. In fact, for $z_3 = 0$ system (6) restricted to the $z_1 z_2$–plane is given by

$$\begin{cases} \dot{z_1} &= -z_1(c z_1 + d z_2) =: f_1(z_1, z_2), \\ \dot{z_2} &= z_2(z_1 - z_2) =: f_2(z_1, z_2). \end{cases} \tag{7}$$

The following result may be derived.

Proposition 2 The unique equilibrium point $(0, 0)$ of system (7) is stable.

Proof Denote $r = \sqrt{z_1^2 + z_2^2}$. Then $\lim\limits_{r\to 0} \dfrac{f_1(z_1, z_2)}{r} = 0 = \lim\limits_{r\to 0} \dfrac{f_2(z_1, z_2)}{r}$. So, according to Theorem 4.1 on page 91 of [22], the equilibrium point $(0, 0)$ of system (7) is stable.

The flow in the local chart V_2 is exactly the same as the flow in the local chart U_2, because the compactified vector field $p(X)$ in V_2 coincides with the vector field $p(X)$ in U_2 multiplied by $(-1)^{n-1}$, where $n = 2$ is the degree of system (1).

4.1.3 In the local charts U_3 and V_3

The expression of the Poincaré compactification $p(X)$ of system (1) in the local chart U_3 has the form

$$\begin{cases} \dot{z_1} &= (e-b) z_1 z_3 + a z_2 z_3 - (1+c) z_1^2 + (1-d) z_1, \\ \dot{z_2} &= (e-1) z_2 z_3 + z_1 z_3 - z_1 z_2 + z_2, \\ \dot{z_3} &= e z_3^2 - z_1 z_3 + z_3. \end{cases} \tag{8}$$

For $z_3 = 0$, system (8) becomes the following system

$$\begin{cases} \dot{z_1} &= z_1[(1-d) - (1+c) z_1], \\ \dot{z_2} &= z_2(1 - z_1). \end{cases} \tag{9}$$

Similar to the case for U_1 in 4.1.1, we consider two cases: (i) $d = 1$, (ii) $d \neq 1$.

(i) If $d = 1$, then I_0 is a unique equilibrium point of system (8) with three eigenvalues $\lambda_1 = 0$ and $\lambda_{2,3} = 1$. So I_0 is a non-hyperbolic equilibrium point with a 1D W^c_{loc} and a 2D W^u_{loc}. Further, it remains to analyze the dynamics of system (8) for $z_3 > 0$ small in the 1D W^c_{loc} related to I_0. This is done in the next proposition.

Proposition 3 When $d = 1$, I_0 is stable along its 1D W^c_{loc}.

Proof It follows from $\lambda_1 = 0$ that system (8) associated to the singular point I_0 has a 1D center manifold. It is the graph of a function $h : \mathbb{R} \to \mathbb{R}^2$ given by $(z_2, z_3) = h(z_1) = (h_1(z_1), h_2(z_1))$ satisfying the conditions

$$h(0) = (0,0), \qquad Dh(0) = (0,0) \tag{10}$$

and

$$\dot{z_2} - Dh_1(z_1)\dot{z_1} = 0, \qquad \dot{z_3} - Dh_2(z_1)\dot{z_1} = 0. \tag{11}$$

The flow on this center manifold is governed by the following one dimensional equation

$$\dot{z_1} = (e-b)z_1 h_2(z_1) + a h_1(z_1) h_2(z_1) - (1+c)z_1^2.$$

To understand the flow on this manifold we expand h in Taylor series around $z_1 = 0$ and obtain

$$h_1(z_1) = \sum_{i=2}^{\infty} a_i z_1^i \quad \text{and} \quad h_2(z_1) = \sum_{i=2}^{\infty} b_i z_1^i,$$

where we have used (10). The use of the condition (11) and the expressions for $\dot{z_1}$ and $\dot{z_2}$ in system (8) produces $a_i = b_i = 0$ for all $i \geqslant 2$, i.e.,

$$h_1(z_1) = 0 \quad \text{and} \quad h_2(z_1) = 0.$$

And so the flow on this manifold is governed by the equation $\dot{z_1} = -(1+c)z_1^2$, which implies that I_0 is locally stable along its center manifold because $z_1 > 0$ in the local chart U_3 and $c > 0$.

(ii) If $d \neq 1$, $I_2\left(\dfrac{1-d}{1+c}, 0, 0\right)$ is the other equilibrium point of system (8) except I_0. Its corresponding three eigenvalues are $\lambda_1 = d-1$ and $\lambda_{2,3} = \dfrac{c+d}{1+c}$. Therefore, I_2 is a saddle-node if $0 < d < 1$, whereas it is an unstable node if $d > 1$. At this time, the eigenvalues associated I_0 are $\lambda_1 = 1-d$ and $\lambda_{2,3} = 1$. So I_0 is a saddle-node if $d > 1$, but an unstable node if $0 < d < 1$.

The flow in the local chart V_3 is the same as the flow in the local chart U_3 by reversing the time. So by the same type of analysis as stated above, using $z_3 < 0$ near the infinity in the local chart V_3 (see $\mathbf{Remark\ 1}$), we get the same result.

4.2 Dynamics of system (1) on the sphere at infinity

Putting together the analysis formulated in the previous subsections one has a global picture of the dynamical behavior of system (1) on the sphere at infinity. The system (1) has two unstable node in the positive and negative endpoints of the x–axis and two unstable centers with 1D W^u_{loc} and 2D W^s_{loc} in the positive and negative endpoints of the y–axis. Further, when $0 < d < 1$, system (1) has two equilibria in the positive and negative endpoints of the z–axis, which are two saddle–nodes; there are also infinitely many saddle–node points with a 1D W^s_{loc} and a 2D W^u_{loc} respectively; when $d \geqslant 1$, system (1) has the two non-hyperbolic equilibria in the positive and negative endpoints of the z–axis, both unstable with a 1D W^s_{loc} and a 2D W^u_{loc}, See Fig.1. This displays Theorem 1.

We observe that the description of the complete phase portrait of system (1) on the sphere at infinity is possible because of the invariance of this set under the flow of the compactifield system.

4.3 Infinite heteroclinic orbit

For $a \leqslant b$ and $0 < d < 1$, the complex dynamical behavior of $O(0,0,0)$ has been discussed in [21]. It is easy to check that the z–axis is invariant under the flow of system (1), and it follows from the calculations above that the origin is asymptotically stable along this axis. Moreover, the equilibria at the endpoints of the z–axis on the sphere at infinity, which coincide with the origin I_0 in the local charts U_3 and V_3, are unstable (see Subsection 4.1.3). Thus system (1) has two infinite heteroclinic orbits as in [14, 17], one of them consisting of the origin $O(0,0,0)$, the positive portion of the z–axis and of one equilibrium on the sphere at infinity (the endpoint of the positive z–axis); the other one consists of the origin, the negative part of the z–axis and of the endpoint of the negative z–axis. Particularly, they are shown in Fig.1 and Fig.2.

These discussions finish the proof of Theorem 2.

5 Conclusion

In this paper, after the local stability of equilibrium point E_1 of a stage-structured predator–prey model is formulated in the critical case $a = b + ce$, a global analysis at infinity of this model is mathematically presented, including a complete description of the phase portrait on the Poincaré sphere at infinity. This mathematical analysis leads to two new discoveries:

(1) The parameter d in this model having no effect on finite dynamical behaviors of this system bears on the dynamical behaviors at infinity of this system;

(2) There exist two infinite heteroclinic orbits in this model.

It is hoped that the investigations of this paper will be beneficial for further studies for similar stage-structured predator–prey models, especially with biological significance.

References:

[1] Chen L, Chen J. Nonlinear Biological Dynamic Systems [M]. Beijing: Science Press, 1993.

[2] Chen L. Mathematical Models and Methods in Ecology [M]. Beijing: Science Press, 1988.

[3] Hofbauer J, Sigmund K. Evolutionary Games and Population Dynamics [M]. Cambridge: Cambridge University, 1998.

[4] Freedman H I. Deterministic Mathematical Models in Population Ecology [M]. New York: Marcel Dekker, 1980.

[5] Murray J D. Mathematical Biology [M]. 2nd corrected Ed. Heidelberg: Springer Press, 1993.

[6] Takeuchi Y. Global Dynamical Properties of Lotka–Volterra Systems [M]. Singapore: World Scientific, 1996.

[7] May R M. Stability and Complexity in Model Ecosystems [M]. Princeton: Princeton University, 1975.

[8] May R M. Theoretical Ecology, Principles and Applications [M]. Oxford: Blackwell, 1981.

[9] Takeuchi Y, Oshime Y, Matsuda H. Persistence and periodic orbits of a three-competitor model with refuges [J]. Math Biosci, 1992, 108(1):105-125.

[10] Matsuda H, Namba T. Toshiyuki co–evolutionarily stable community structure in a patchy environment [J]. J Theoret Biol, 1989, 136(2):229-243.

[11] Aiello W G, Freedman H I. A time delay model of single–species growth with stage structure [J]. Math Biosci, 1990, 101:139-153.

[12] Aiello W G, Freedman H I. Analysis of a model representing stage-structured population growth with stage-dependent time delay [J]. Siam Appl Math, 1992, 52:855-869.

[13] Wang W, Chen L. A predator–prey system with stage structure for predator [J]. Comput Math Appl, 1997, 33(8):83-91.

[14] Messias M. Dynamics at infinity and the existence of singularly degenerate heteroclinic cycles in the Lorenz system [J]. J Phys A: Math Theor, 2009, 42(11):115101.

[15] Messias M. Dynamics at infinity of a cubic Chua′s system [J]. Internat J Bifur Chaos, 2011, 21(01):333-340.

[16] Llibre J, Messias M. Global dynamics of the Rikitake system [J]. Physica D Nonlinear Pheonomena, 2009, 238(3):241-252.

[17] Liu Y. Dynamics at infinity and the existence of singularly degenerate heteroclinic cycles in the conjugate Lorenz–type system [J]. Nonlinear Analysis Real World Applications, 2012, 13(6):2466-2475.

[18] Geng F, Li X. Singular orbits and dynamics at infinity of a conjugate Lorenz-like system [J]. Math Modelling and Anal, 2015, 20(2):148-167.

[19] Wang H J, Li X Y. More dynamical properties revealed from a 3D Lorenz-like system [J]. Int J Bifur Chaos, 2014,24(10):1450133.

[20] Cima A, Llibre J. Bounded polynomial vector fields [J]. Trans Amer Math Soc, 1990,318(2):557-579.

[21] Zhang X, Chen L, Neumann A U. The stage–structured predator–prey model and optimal harvesting policy [J]. Math Biosci, 2000, 168(2):201-210.

[22] Zhang Z, Ding T, Huang W, et al. Qualitative Theory of Ordinary Differential Equations [M]. Beijing:Science Press, 1985.

(责任编辑：郁 慧)